ISSN: 0974-5823 Vol. 6 No. 3 December, 2021

International Journal of Mechanical Engineering

Effect of relative groove position on performance analysis of heat transfer enhancement in solar air heater using Numerical approach

Amit Kumar[1*], Dheeraj Kumar[1], Kundan Kumar[1] and Apurba Layek[1]

[1] National Institute of Technology-Durgapur, Mechanical engineering department, India

Abstract

The present article represents the investigation based on numerical technique for the roughened solar air heater consisting of chamfered ribs with groove$_i$ on the surface plate approaching towards computational fluid dynamics (CFD)$_{fluent}$ approach. The required input parameter$_i$ for 2-D (CFD)$_{fluent}$ model for the analysis taken as relative$_i$ groove$_i$ position (g/P) of 0.3,0.4,0.5 and 0.6, relative$_i$ *roughness$_s$* pitch$_i$ (P/e) of 4.5,6,8,10 keeping relative$_i$ *roughness$_s$* height (e/D) and chamfered angle (φ) of 18^0 constant at different values of Reynolds number varies between 5000-20000.Using *artificial roughness$_s$* on the absorber surface, rate of heat transfer increases as comparing to smooth channel. The computational results on the basis of K-ξ turbulence model is validated with those of existing experimental values working under the same flow conditions. The results signify the impact of design parameter$_i$ on different thermal properties like average Nusselt$_i$ number and friction factor$_i$ showing enhancement in Nusselt$_i$ number and attain maxima at g/P of 0.4 and P/e of 6 for all value of Reynolds number specifically due to more no of reattachment point of free shear layer between the consecutive ribs. Thus, the range investigated and the type of rib arrangement on the absorber surface shows the strong function of Nusselt$_i$ number with its maximum value of heat transfer.

Keywords: *CFD, Chamfered rib, Solar air heater (SAH), Heat Transfer*

1. Introduction

As solar energy is known to be one of the most important non-conventional source of energy in which the energy from the sun captured for generation of heat in many industrial application as well as clean resources like food processing industry, leather manufacturing industry, chemical, rubber, salt production, textiles, fruits and vegetable for drying application, fish and marine products, spices, etc are progressively acquired for heating purpose.The solar air heater is a basic equipment used for the heating of air which is known to be less efficient due to low rate of heat transfer coefficient$_i$ between the flowing fluid and the absorber surface [1].To make the solar air heater system more efficient$_t$, the artificial *roughness$_s$* used on the absorber surface which enhance the heat transfer capability$_y$ of the system. Till date large number of experimental and computational investigation has been performed by many researches and it is seen that artificial *roughness$_s$* on the absorber surface greatly improves the solar air heater performance comparing to the smooth channel [2]. Karmare and Tikerkar [3] did the computational analysis on arc shaped artificial roughness$_s$ on the surface plate and get the heat transfer and friction characteristics using FLUENT 6.3.26 (CFD)$_{fluent}$ code. Numerical analysis conducted by Yadav et al. [4] for the square-shaped ribs on the surface plate and observed that relative$_i$ roughness$_s$ height i.e. e/D known to be an important parameter$_i$ used for the enhancement of heat transfer rate. Bolemtafes and Benzaoui [5] did the (CFD)$_{fluent}$ analysis on solar air heater for the roughened surface based on different turbulence model.Chaube et al. [6] investigated the different type of roughness$_s$ geometry like square, trapezoidal,rectangular, circular, rectangular, triangular etc using numerical approach and found that the highest values obtained for rectangular ribs which justified with existing experimental results. Webb and Eckert [7] did the analysis on the square-shaped roughened material and investigated that the relative$_i$ roughness$_s$ pitch$_i$ (P/e) < 8 does not create strong point of reattachment$_t$ at free shear layer very adjacent to it. . Kumar and Saini [8] did the analysis on the on arc-shaped geometry using (CFD)$_{fluent}$ approach to understand the flowing fluid behavior and heat transfer characteristics of a solar air heater. Gupta et al. [9] did the analysis on solar air heater design to understand the fluid flow$_i$ behaviour and thermal characteristics of the transitionally roughened type flow regime. Kumar and Layek [10] having circular-shaped ribs on the absorber surface to get the optimal condition of heat transfer. Kumar et al. [11-12] did the numerical analysis on solar air heater having chamfered ribs on the absorber surface to get the effect of heat transfer based on the parametric condition. Similar type of study can be seen for the circular and square shaped roughened surface as discussed by Kumar et al. [13-14]. Layek et al. [15] conducted experimental investigation$_n$ on chamfered ribs with groove$_i$ used as a *roughness$_s$* element on the absorber plate to get its maximum value on heat transfer and friction at chamfer angle of 18^o for the given parameter$_i$.From the previous study, it is observed that some parameter$_i$ used required accuracy and very difficult to test experimentally, requires massive cost, as well as time also and such problem can be corrected by using the simulation technique.

The primary goal of work is to show (CFD)$_{fluent}$ can be successfully used to design solar air heater primarily based on their overall thermal performance.This work generally deals to understand the effect of transverse Chamfered rib- groove$_i$ *roughness$_s$* on the basis of numerical study.An attempt$_t$ has been done to know the effect$_t$ of relative$_i$ groove$_i$ position (g/P) of 0.3,0.4,0.5 and 0.6 and relative$_i$ *roughness$_s$* pitch$_i$ (P/e) of

4.5,6,8,10 by putting relative$_i$ *roughness$_s$* height (e/D) and chamfer angle (φ) constant on the enhancement$_t$ of heat transfer and friction characteristics of solar air heater. Keeping entire geometric as well as operating parameteric condition similar to the earlier experimentally conducted work by Layek et al [15]. The experimentally observed data of Layek et al [15] is used for the validation$_n$ from of present numerical investigation.

2. Artificial *roughness$_s$* and its concept

The turbulent flow inside the channel is vey much desirable to enhance the heat transfer capability$_y$ of a solar air heater system.This enhancement is possible only by approaching towards *artificial roughness$_s$* over the surface plate keeping the rib height very small as comparison the duct height.The laminar$_r$ sub layer very adjoint to plate create thermal resistance$_e$ to convective heat transfer coefficient$_t$,so it is very necessary to break this viscous sub layer by the *roughness$_s$* element on the absorber surface greatly improves the turbulence effect of the flowing stream.Therefore, *artificial roughness$_s$* is known to be an efficient technique generally used for their enhanceing the heat transfer capability of solar air heater duct.Different parameter$_i$ that are characterized on the basis of its shape and sizes of the roughness i.e. rib height (e) and pitch$_i$ (P) are considered to be an impotant one.Generally,these parameter$_i$ are specified as non-dimensional parameter$_i$ such as relative$_i$ *roughness$_s$* pitch$_i$ (P/e), relative$_i$ *roughness$_s$* height (e/D),attack angle (α) , relative$_i$ gap width (g/e) etc.

3. CFD Simulation

3.1 Solution domain

The required domain used for the (CFD)$_{fluent}$ analysis recommended by ASHRAE standard [16] consisting of the three basic regions naming entrance section L_1, test section L_2 and exit section L_3 as represented in Fig.1. In this analysis the test section is equipped with chamfered ribs as a *roughness$_s$* element consisting of constant value of heat flux i.e.,1000 W/m2. The result thus acquired from the simulation approach for Nusselt$_i$ number and friction factor$_i$ has been used to validate those results with experimentally available result of Layek et.al [15]. Table 1 Shows the detail of *roughness$_s$* geometry used for numerical analysis.

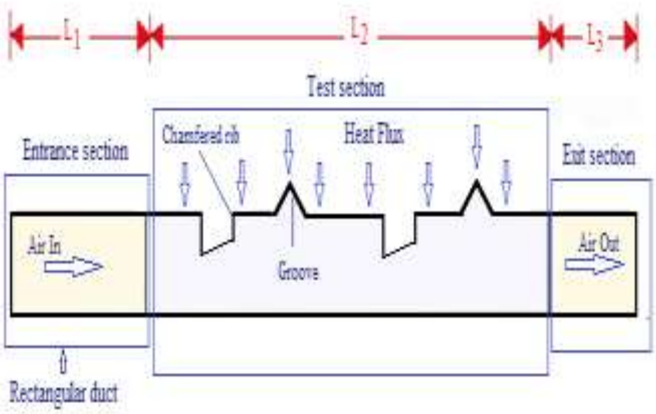

Fig.1: 2D Computational Domain for solar air heater

3.2 Two-Dimensional Model Description and roughness$_s$ geometry

The 2-D numerical study accomplished to understand the impact of heat transfer and friction characteristics for artificially roughened surface of a solar air heater. If the ribs geometry is straight forward than the 2D version is very a great deal for the analysis of floww through the channel acquiring the same computation time and energy. (CFD)$_{fluent}$ simulation code (ANSYS FLUENT 16.2) has been volved to solve the conservation equation of mass, momentum, and energy. The software SOLID WORKS v 2015 has been used for the advent of the required geometry which includes a primary method for the entire running of the model. The dimensionless parameter$_i$ consisting of different values relative$_i$ groove$_i$ position (g/P) along with relative$_i$ *roughness$_s$* pitch$_i$ (P/e) at constant relative$_i$ *roughness$_s$* height (e/D) evaluated for all ranges of Reynolds number. The schematic diagram of ribs and its geometry on the roughened surface are depicted in Fig.2.

The following important assumptions must be achieved for the analysis:

(1)The fluid flow must be Steady,2-dimensional and fully developed.

(2) Homogeneous and isotropic throughout the wall.

(3) Thermal conductivity of duct wall and absorber surface material are temperature independent.

(4) Wall should be no-slip boundary circumstance.

(5) Heat loss through radiation must be negligible.

Table 1: Operating and geometrical parameter$_i$ used for CFD analysis

Operating and Geometrical parameter$_i$	**Value / Range**
Test$_t$ length, L_2	1200 mm
Entrance$_e$ length, L_1	800 mm
Exit$_t$ length, L_3	600 mm
Duct width, W	150 mm
Height, Duct H	30 mm
Hydraulic diameter, Duct, D	50 mm
Constant heat flux$_x$, q"	1000 W/m^2
Reynolds number	5000-20000
Relative$_i$ *roughness$_s$* pitch$_i$, (P/e)	4.5,6,8,10
Relative$_i$ groove$_i$ position (g/P)	0.3,0.4,0.5,0.6
Chamfer angle (φ)	18^0

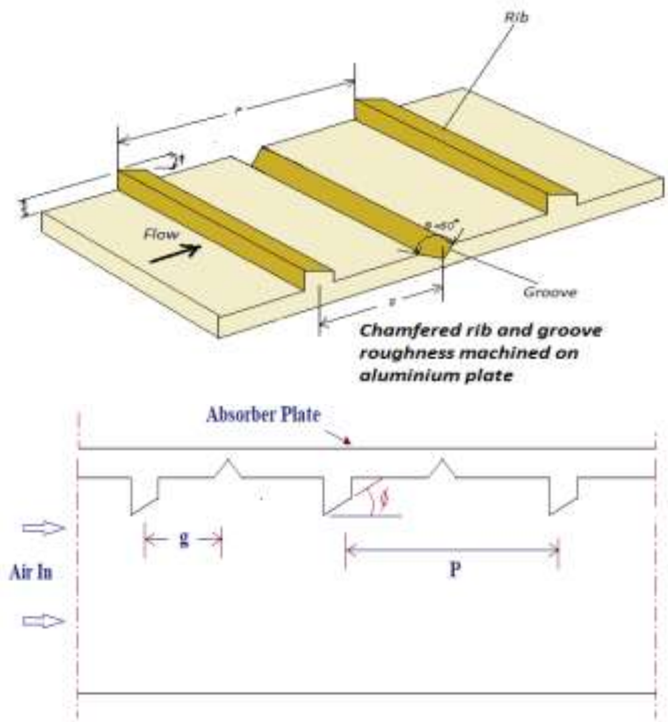

Fig.2: Schematic Sketch diagram of Chamfered Rib Geometry

3.3 Generation of mesh

The meshing has been done on commercially accessible ANSYS fluent software. The geometry͡ which is created thus imported into the ANSYS mesh. To attain uniform rectangular mesh shaped cells approaching to get the best orthogonal quality, the mapped face option has been operated. Finally͡, mesh was generated by way of clicking on "Generate Mesh" button. Fig.3 indicates the meshed area for different cases. The meshed domain consisted typically of non-uniform sized cells. Fine meshing became completed close to the walls in order to solve the involved governing differential equations appropriately inside the laminar$_r$ sub-layers at these areas.The mesh size decreases towards the adiabatic wall.

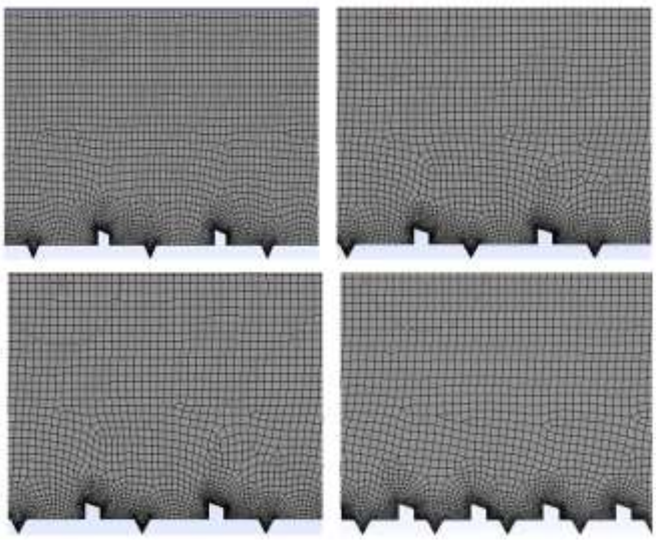

Fig.3: 2-dimensional meshing of transverse chamfered rib groove$_i$ for different value of pitch$_i$ and relative$_i$ groove$_i$ position

4. Results & Discussion

The outcomes thus calculated based on $(CFD)_{fluent}$ analysis for the roughened plate of solar air heater must be equated to those with the smooth one in order to get the heat transfer and friction characteristics corresponding to the same flow condition. The consequences of the Nusselt$_i$ number and friction factor$_i$ observed for the smooth channel has been validated with the modified equation of Dittus-Boelter$_i$ equation [17] and Blasius equation [18] respectively as represented in Fig. 4.

$Nu_s = 0.023Re^{0.8}\ Pr^{0.4}$: Dittus-Boelter$_i$ equation (1)

$f_s = 0.079\ Re^{-0.25}$: Blasius equation (2)

Nusselt$_i$ number defined as;

$Nu = hD/K$ (3)

Friction factor$_i$ given as,

$f_r = (\Delta P/l)\ D/2\rho V^2$ (4)

where ΔP/l, Pressure drop along the channel.

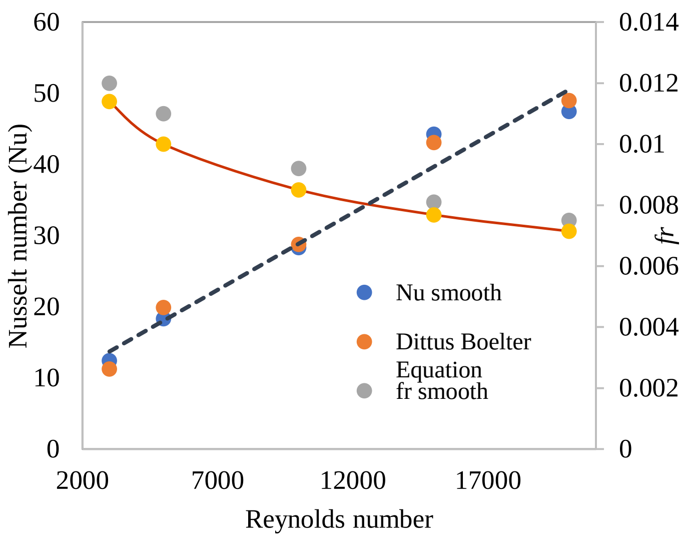

Fig.4: *Nu*, *fr* variation for the smooth duct.

The numerical analysis is carried out for the required roughened ssurface of a solar air heater (SAH) consisting of transverse chamfered rib- groove$_i$ *roughness$_s$* embedded over the absorber surface and its flow characteristics are presented in the present analysis. The analytical results observed from the present computational fluid dynamics $(CFD)_{fluent}$ approach are validated with those of earlier experimental data investigated by Layek et al. [15] working under same operating and flowing conditions. The outcome data which are available from the experimental investigation has been used for the best suitability of the turbulence model. The contour profile view of a velocity͡ vector and velocity͡ magnitude at different groove$_i$ positions (g/P) of 0.3,0.4,0.5 and 0.6 at P/e of 6 are represented in Fig.5.

4.1 Effect of relative$_i$ pitch$_i$ ratio (P/e)

The simulation with various geometrical *roughness$_s$* configurations is carried to evaluate the outcome of relative$_i$ pitch$_i$ ratio on Nusselt$_i$ number. Fig. 6, depict the behaviour of relative$_i$ *roughness$_s$* pitch$_i$ ratio (P/e) on Nusselt$_i$ number for entire range of Reynolds number keeping geometrical parameter$_i$ as constant i.e., e/D_h = 0.04 and ϕ = 18°. It is observed that maximum reattachment points of free shear layer occurred at relative$_i$ *roughness$_s$* pitch$_i$ (P/e) of 6 results higher value of heat transfer rate over the heated plate. The friction factor$_i$ variation as depicted in Fig. 7, for different range of P/e, g/P = 0.4, e/D_h = 0.04 and ϕ = 18°. It is noticed that the friction factor$_i$ tend to decrease with increase in Reynolds number. This can be explained that with the rise in Reynolds number results an increase of transition to turbulence which may occur at a downstream and suppression of boundary layer thickness results the decrease in friction factor$_i$.

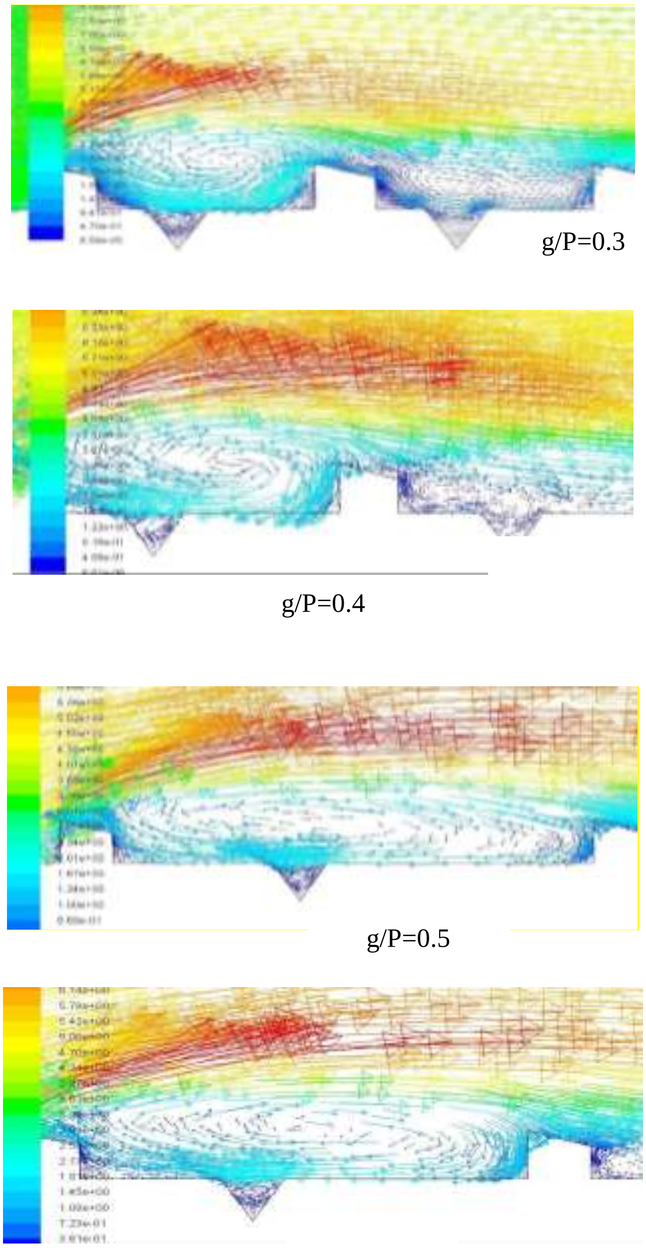

Fig: 5: Images of the Velocity vector and velocity magnitude at different groove$_i$ positions (g/P)

4.2. Effect of relative$_i$ groove$_i$ *position (g/P)*

The simulation with various geometrical *roughness$_s$* configurations is carried to evaluate the effect of relative$_i$ groove$_i$ position on Nusselt$_i$ number. Fig. 8, shows the effect of relative$_i$ groove$_i$ position (g/P) on Nusselt$_i$ number keeping other geometrical parameter$_i$ as constant i.e., P/e = 6, e/D_h = 0.04 and ϕ = 18°. It is observed that maximum reattachment points of free shear layer occurred at relative$_i$ *roughness$_s$* groove$_i$ of 0.4 results maximum heat transfer rate over the heated plate. It is observed, the Nusselt$_i$ number initially tend to increase by increasing with relative$_i$ groove$_i$ position (g/P) and reaches its optimum value at g/P = 0.4, and then further increase of (g/P) it decreases. It is because after certain limit of relative$_i$ groove$_i$ position level of turbulence is decrease as number of groove$_i$ also decrease and optimum value of Nusselt$_i$ number attain at relative$_i$ groove$_i$ position at 0.4. Fig.10 depict the Nusselt$_i$ number enhancement ratio on the basis of different value of Reynolds number

ranges from 5000-20000 and it depict its optimum result of Nusselt$_i$ number enhancement$_i$ ratio found to be 3.68 times in comparison to smooth channel at constant (e/D) of 0.04 and (P/e) of 6 corresponding to highest value of Reynolds number i.e., 20000. Fig.9 shows average friction factor$_i$ against relative$_i$ *roughness$_s$* groove$_i$ (g/P) for entire range of Reynolds number at P/e = 6, e/D_h = 0.04 and ϕ = 18°. It is observed that the rib roughened surface of chamfered shaped with groove$_i$ on it yield higher value of friction factor$_i$ mainly due to repetitive chamfering of the ribs and the additional generation of vortex by the groove$_i$ causes greater eviction of heat from the surface as well as lead to frictional loss.

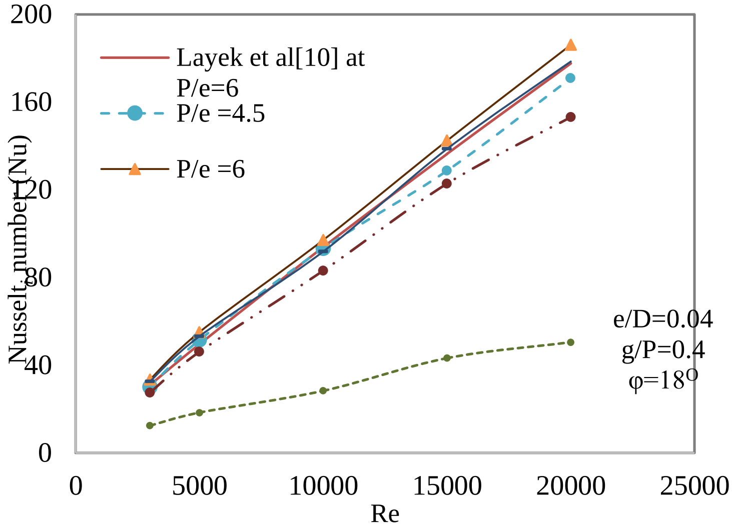

Fig: 6: Nu variation w.r.t Reynolds number

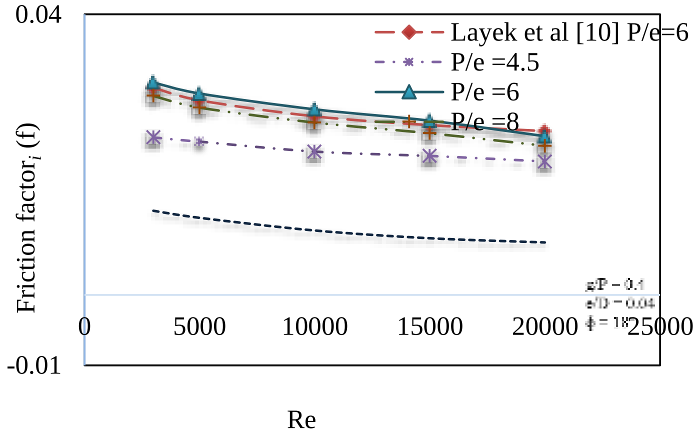

Fig: 7: *fr* variation w.r.t Reynolds number

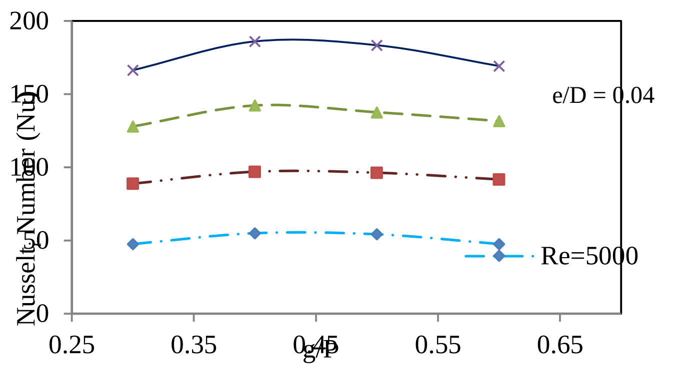

Fig: 8: Effect of g/P on Nu for entire range of Re at P/e = 6, e/D_h = 0.04 and ϕ = 18°

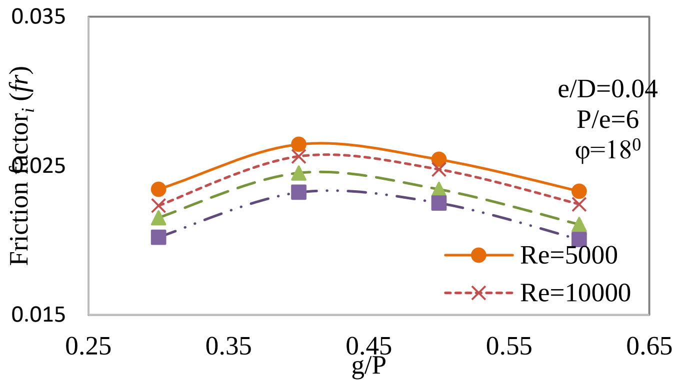

Fig: 9: Effect of g/P on *fr* for entire range of Re at P/e = 6, e/D_h = 0.04 and ϕ = 18°

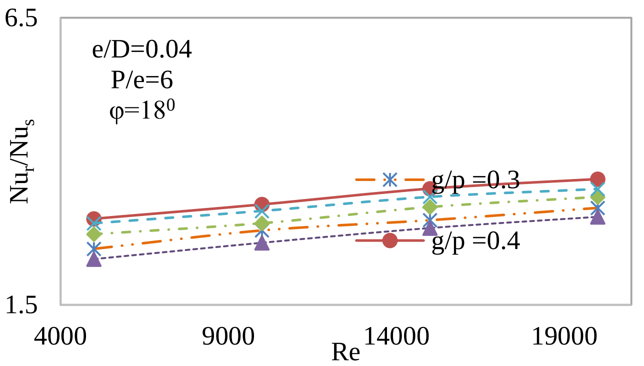

Fig: 10: Effect of g/P on Nusselt$_i$ number enhancement ratio (Nu_r/Nu_s) at ϕ = 18°

5. Conclusions

For the required geometry 2-dimensional numerical study has been done approaching towars to analyse the effect$_t$ of heat transfer enhancement on transverse$_e$ chamfered rib- groove$_i$ *roughness$_s$* on the absorber surface of a solar air heater$_r$. A numerical analysis is carried out to developed rectangular duct model through computational fluid dynamics$_s$ (CFD)$_{fluent}$. The shapes of chamfered rib- groove$_i$ sectioned arranged in different position in-line arranged on bottom walls of the rectangular solar air heater$_r$ duct.The output of numerical simulations has been drawing to the following conclusions:

- The heat$_t$ transfer enhancement and friction characteristics due to chamfered shaped rib *roughness$_s$* corresponding to ranges studied acquired from the (CFD)$_{fluent}$ analysis in comparison to the smooth channel which depict approximately very close value corresponding to experimental result.
- The above cases studied for all the required geometric and parametric condition,the Nusselt$_i$ number tends to rise by increasing Reynolds number.
- The optimum values obtained for Nusselt$_i$ number (Nu) and friction factor$_i$ (fr) for the chamfered ribs at P/e of 6 at constant relative$_i$ groove$_i$ position of 0.4 and fixed chamfered angle of 18° are found to be 186.06 and 0.02952 respectively.
- The optimum value of heat transfer gain achieves at relative$_i$ groove$_i$ position (g/P) of 0.4 for the given parametric ranges.Similar results is also obtained for the friction factor$_i$, which goes on increasing up to (g/P) of 0.4 and the furthermore increase of g/P value Nusselt$_i$ number decreases.
- The highest value of Nusselt$_i$ number enhancement ratio observed to be 3.68 times in comparison to smooth channel at constant (e/D) of 0.04 and (P/e) of 6 at its maximum flowing condition i.e. Reynolds number of 20000.

Data Availability Statement

All data, models, and code generated or used during the study appear in the submitted article.

Acknowledgement

The authors are extremely grateful to entire fraternity at National Institute of Technology, Durgapur for their constant support, motivation and guidance.

References

[1] Aharwal, Gandhi and saini "Heat transfer and friction characteristics of solar air heater ducts having integral inclined discrete ribs on absorber plate" Heat and mass transfer (2009).

[2] Varun, R. P. Saini, and S. K. Singal, A review on roughness geometry used in solar air heaters, Solar Energy, 81 1340-1350 (2007).

[3] Karmare and Tikerkar "Analysis of fluid and heat transfer in a rib grit roughened surface solar air heater using CFD." Solar energy (2010).

[4] Yadav AS, Bhagoria JL. (2013). Modeling and simulation of turbulent flow through a solar air heater having square-sectioned transverse rib roughness on the absorber plate., Sci World J. (2013) DOI:10.1155/2013/827131.

[5] Bolemtafes and Benzaoui "CFD based analysis of heat transfer enhancement of solar air heater provided with transverse rectangular rib" Energy (2014).

[6] Chaube A., Sahoo P. K. and Solanki S. C., Analysis of heat transfer augmentation and flow characteristics due to rib roughness over absorber plate of a solar air heater, Renewable Energy, 31,317-331(2006).

[7] R.L. Webb, E.R.G. Eckert, R.J. Goldstein., Heat transfer and friction in tubes with repeated rib roughness, Int. J. Heat Mass Transfer,14,601–617 (1971).

[8] Kumar S, Saini RP. CFD based performance analysis of a solar air heater duct provided with artificial roughness. Renewable Energy; 34:1285e91, 2009.

[9] Gupta D., Solanki S. C. and Saini J. S., 1993, Heat and fluid flow in rectangular solar air heater ducts having transverse rib roughness on absorber plates, Solar Energy, 51(1): pp. 31- 37.

[10] Kumar A, Layek A. Nusselt number and fluid flow analysis of solar air heater having transverse circular rib roughness on absorber plate using LCT and computational technique. Thermal Science and Engineering Progress. 2019 Dec 1;14:100398.

[11] Kumar A, Layek A, Kumar D. Effect of relative roughness pitch on the performance evaluation of a solar air heater roughened with chamfered rib and groove roughness on the surface plate using CFD technique.AIP Conference Proceedings 2020 Nov 2 (Vol. 2273, No. 1, p. 050023). AIP Publishing LLC.

[12] Kumar A, Layek A, Mondal PK. Heat Transfer Analysis of a Solar Air Heater Roughened with Chamfered Rib and Groove Roughness on the Absorber Plate Using CFD Approach. InAdvances in Mechanical Engineering 2020 (pp. 1373-1384). Springer, Singapore.

[13] Kumar A, Layek A, Ansu AK, Rawani A. Performance Evaluation of a Solar Air Heater with Transverse Ribs on the Absorber Surface Using CFD Technique. InEnergy Systems and Nanotechnology 2021 (pp. 47-56). Springer, Singapore.

[14] Kumar A, Kumar D, Layek A. Determination of Nusselt Number Over Artificially Roughened Solar Air Heater Using Numerical Approach. Theoretical, Computational, and Experimental Solutions to Thermo-Fluid Systems: Select Proceedings of ICITFES 2020. 2021:483.

[15] Layek A, Saini JS, Solanki SC., Heat transfer and friction characteristics for artificially roughened ducts with compound turbulator. International Journal of Heat and Mass Transfer, 50,4845–4854 (2007).

[16] ASHRAE Standard 93, Method of Testing to Determine the Thermal Performance of Solar Collectors, American Society of Heating, Refrigeration and Air Conditioning Engineers, GA,30329, Atlanta, 2003.

[17] McAdams WH., Heat Transmission. McGraw-Hill, New York, 1942.

[18] Kays W.M., Perkin H. Forced convection internal flow in ducts. In: Rohsenow W.M., Hartnett I.V., editors, Handbook of Heat Transfer. McGraw-Hill, New York.

Nomenclature

D	hydraulic diameter size, (m)
e	rib height, (mm)
e/D	$relative_i$ *$roughness_s$* height
g/P	$relative_i$ $groove_i$ position
h	heat transfer coefficient, ($W/m^2 K$)
Re	Reynolds number (dimensionless)
k	thermal conductively, (W/mK)
W	width, Duct (m)
Nu	Nusselt number (dimensionless)
P	$pitch_i$, (mm)
P/e	$relative_i$ *$roughness_s$* $pitch_i$ ratio
V	fluid velocity duct, (m/s)
ρ	density of air, (Kg/m^3)